

A Novel Transverse Flux Generator in Direct-Driven Wind Turbines

Dmitry Svechkarenko, Juliette Soulard, and Chandur Sadarangani
Division of Electrical Machines and Power Electronics
School of Electrical Engineering, Royal Institute of Technology
Teknikringen 33, 10044 Stockholm, Sweden, email: dmitrys@ee.kth.se

Abstract—The higher specific torque and power density of a transverse flux permanent magnet (TFPM) machine in comparison to a conventional machine makes it a promising direct-driven wind turbine generator. The new topology presented in this paper is believed to have a better utilization of the available in the nacelle space. This would favor a reduced inactive weight of the generator and thus remove one of the major obstacles for large wind power units. The new topology is presented together with the analytical model used in the design procedure. The analytical model is used in a parametric study and the first conclusions about the performance of the new TFPM topology are drawn.

I. INTRODUCTION

Wind power is one of the fastest growing sustainable energy resources over the past decade. Due to the increased number of wind turbines installed, the energy production by means of wind power is increasing by approximately 30% annually [1]. This trend is likely to continue even in the future since wind power became more economically beneficial, as the so-called fixed feed-in tariffs (in Germany, Denmark, Spain) and green certificates (in Sweden, UK) were introduced by the governments.

Despite all the recent advances, the average annual wind power penetration level hardly exceeds 5% even in countries with large installed wind capacity [1]. To increase the share of power produced by wind, larger and more reliable power generating units with high availability are required.

Wind turbines with high rated power (≥ 1.5 MW) are primarily intended for the regions with high wind speeds, as the shaft power of turbine is proportional to the cube of wind speed. The wind speeds offshore are often significantly higher than onshore and as a result the offshore installation of large-scale wind farms became a new tendency in wind power development that eventually led to a number of projects, mainly in Europe.

Availability and reliability are the issues of particular importance especially for the offshore wind turbines. However, a gearbox used in conventional wind energy systems is subject to mechanical wear and potential risk of failure. Furthermore, it generates vibration and noise, increases losses and requires more frequent maintenance at considerable expense [2]. In order to avoid these shortcomings and increase reliability, a gearless wind energy system for direct-driven generators has been introduced and successfully being manufactured since 1991 [3]. However, for the grid connection of a gearless system, an electric power converter for the full rated power

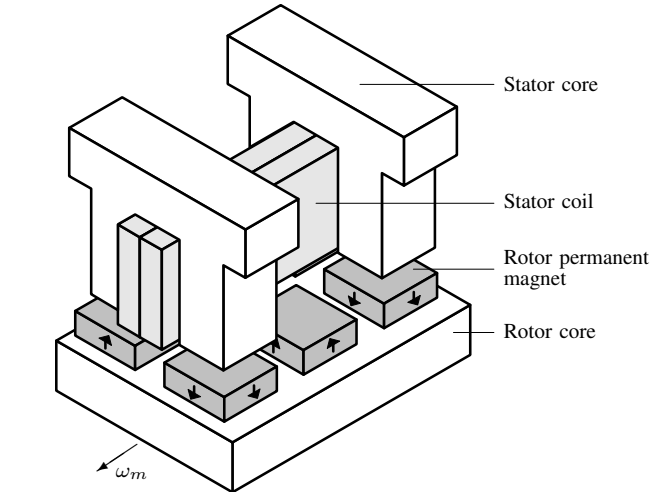


Fig. 1. Transverse flux permanent magnet topology, where w_m is the direction of movement.

is required. This introduces extra cost and additional losses. Yet the efficiency of such a system can be somewhat higher than the efficiency of the system containing a gearbox and an induction generator directly connected to the grid [4]. Another advantage of fully-rated converter is that it allows variable turbine speed, which results in increased energy yield.

A number of studies have been conducted to examine different types of generators suited for direct-driven wind turbine applications. In [4], it was found that the permanent-magnet synchronous generator can be a best suited solution for this purpose. The further analysis presented in [3], showed that the weight of direct-driven permanent magnet generator is approximately half of electrically excited one, yet the energy yield is higher. Reduced magnet prices in the last years have made permanent magnet machines more feasible. In [4] and [5], different topologies of permanent magnet synchronous generators were investigated. In both works, a transverse flux topology of wind generators was considered to be a promising solution particularly suited for the low-speed direct-driven wind energy systems.

A. Transverse Flux Topology

The transverse flux permanent magnet (TFPM) topology shown in Fig. 1 owes its name to the fact that the flux lines

are in a perpendicular (transversal) plane to the direction of movement and the flow of the torque producing current. The main benefit of using this topology is an available high torque density [6]. Thanks to the global windings, by increasing the number of poles, the current loading can be increased and as a result a higher value of specific torque density can be achieved [7]. Another attractive feature of a TFPM is that it allows current and magnetic loading to be set independently, resulting in a more favorable construction as magnetic circuit and armature winding designs are decoupled.

One of the most important drawbacks of a TFPM is its high flux leakage, resulting in a poor power factor. The amount of leakage flux can be diminished to a certain extent by increasing the pole width at the cost of reduced torque density. Therefore, the machine designer has to consider this compromise between power factor and torque density and find an optimal solution [8]. Another significant disadvantage of a TFPM is the complicated mechanical structure of the magnetic circuit, which consist of a large number of small size components. A number of various topologies of TFPM were presented and described in the literature, since it first drew the attention of machine designers in the mid-80s [9]. Nevertheless, the research in this area continues and new topologies are being introduced.

The novel TFPM topology presented in this paper has a better utilization of the available volume and can likely decrease inactive weight, which makes it especially attractive for the use in wind turbines.

II. NOVEL TFPM DESIGN

The machine can be refer to as a rotational multi-phase single-sided transverse flux machine without return paths [6], [7]. The cross-section of the novel TFPM generator geometry is presented in Fig. 2. As can be observed, the generator consists of a hollow toroidal rotor with surface-mounted permanent magnets embraced by the laminated stacks with the windings placed in the slots. The main machine radius R_m and the tube radius R_s are shown in Fig. 2. The cut required for the mechanical assembling of the rotor on the shaft is presented by angle 2ξ .

In order to easier identify the location of machine dimensions and simplify further analysis, the subscripts 's' and 'r' were introduced in the notations, which stand for the stack plane and rotational (peripheral) plane, respectively.

The number of stator teeth per stack Q_s should be a multiple of the number of phases (in this configuration selected to be 3) and a multiple of 2 in order to ensure the closed paths for the flux generated by the magnets of opposite polarity. Due to the introduced cut, the lateral slots contain only one winding.

A. Magnetic Design

The high current loading allowed in a TFPM could result in considerable values of armature reaction that cause eddy current losses. For these purpose, the iron parts should be made of laminated material. Moreover, the original idea of TFPM implies that the magnetic fluxes should be carried in

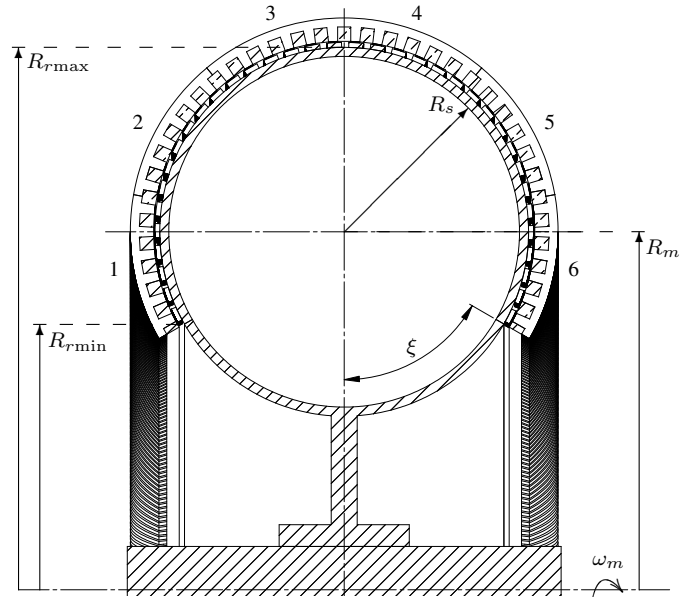


Fig. 2. Cross-section of the novel TFPM generator in the stack plane with the main dimensions.

planes transversal to the direction of movement. The laminated material would likely decrease the flux flow in the rotational direction and the fringing effects. In addition, the manufacturing of stacks in laminations is a more common way in electrical machine production.

The main dimensions of the generator in the stack and rotational planes are presented in Fig. 3. For simplicity, this figure depicts the machine in a linear representation.

The toroidal shape of the generator may create a non-equal flux distribution in different slots, which results in unbalanced induced electromotive force (emf). In order to reduce this effect, the magnet and/or stack dimensions in rotational plane should be scaled in such a way that each magnet induces nearly the same amount of emf in the winding per stack per slot. Therefore, the magnet angle $\alpha_{m,r}$ (see Fig. 6) in the rotational plane should be kept constant.

$$\alpha_{p,r} = \frac{2\pi}{p}, \quad (1)$$

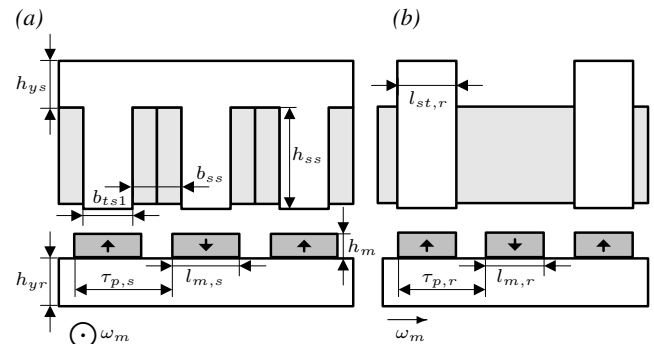


Fig. 3. Schematic representation of the generator in the stack (a) and rotational (b) planes.

$$\tau_{p,r} = \alpha_{p,r} R_r, \quad (2)$$

where p is the number of poles and R_r is the radius on the rotor surface. As it can be observed in Fig. 2, the radius R_r varies depending on the position on the rotor surface, thus the pole pitch $\tau_{p,r}$ varies as well. The radius R_r for each tooth can be calculated as

$$R_r(i) = R_m - R_s \cos \left[\left(i - \frac{1}{2} \right) \alpha_{p,s} + \xi \right], \quad (3)$$

where i changes between $1..Q_s$. As shown in Fig. 2, $R_{r\min}$ corresponds to $i = 1$, whereas $R_{r\max}$ to $i = Q_s/2$. The mechanical pole angle $\alpha_{p,s}$ in the stack plane is given by

$$\alpha_{p,s} = \frac{2\pi - 2\xi}{Q_s}. \quad (4)$$

However, to manufacture $Q_s/2$ magnets each with different thickness would considerably increase their cost. Furthermore, it would be difficult and expensive to manufacture stacks with a varying thickness. It was therefore suggested that the stacks could be divided into sectors (6 sectors are shown in Fig. 2), while the thickness of each sector is kept constant. The magnets thickness follows the stack thickness, which implies a slight variation in $\alpha_{m,r}$. The number of teeth per sector should be a multiple of 6 and the number of sectors should be selected even. This reduces the number of magnets of different thickness to $Q_s/12$.

For the desired maximum value of the flux density B_g in the airgap of length g , the magnet height is obtained by

$$h_m = \frac{\mu_{pm} g}{\frac{B_{r,pm}}{B_g} - 1}, \quad (5)$$

where $B_{r,pm}$ is the magnet remanent flux density and μ_{pm} is the magnet relative permeability. These parameters are specified for the selected type of the permanent magnet material.

By assuming a maximum allowed flux density created by the magnets in the tooth \hat{B}_{ts} and recognizing that the whole flux from the magnets concentrates in the opposite tooth, the required minimum tooth thickness b_{ts1} can be calculated as follows

$$b_{ts1} = \frac{\hat{B}_{r,pm}}{\hat{B}_{ts}} l_{m,s}. \quad (6)$$

In conventional radial-flux permanent magnet machines, the rotor and stator yokes have normally half of a tooth thickness, since the magnetic flux is split after it leaves the teeth. However, this is not the case in TFPM as the yokes carry the complete flux from the teeth. Therefore, the stator yoke should have at least the same thickness as the tooth thickness. If the same maximum flux density is assumed in the all iron parts of machine, the rotor and stator yoke heights can be found as

$$\hat{B}_{ts} = \hat{B}_{ys} = \hat{B}_{yr}, \quad (7)$$

$$b_{ts1} = b_{ys} = b_{yr}. \quad (8)$$

B. Arrangement of Magnets and Windings

The TFPM topology allows to use a stator winding of a simple mechanical structure, which facilitates high voltage insulation. This could be an attractive feature in the future since the voltage of wind generators has been continuously increasing in the past few years and voltage levels up to 5 kV can reasonably be expected in the forthcoming generators [10].

The machine has no common rotating field, although there exist three independent alternating fields shifted by 120 electrical degrees. The shift is created by the magnets mechanically displaced on the rotor surface. Two possible magnets and windings arrangements are presented in Figs. 4 and 5. The flux paths for both cases are shown with a dashed line.

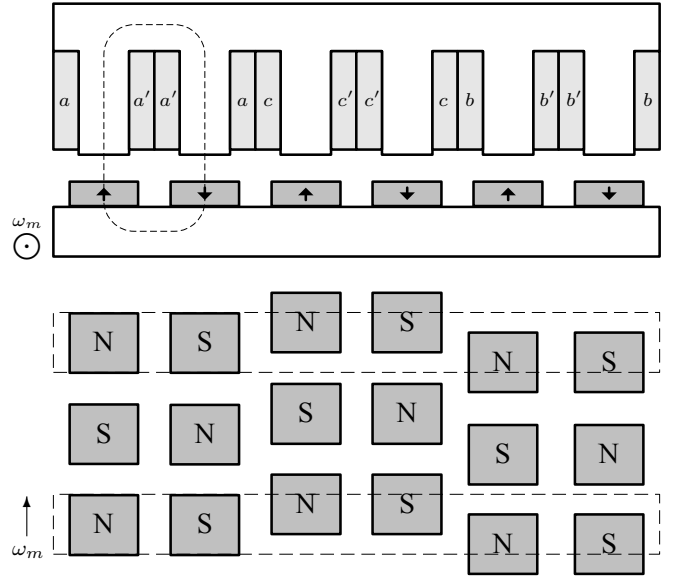


Fig. 4. Arrangement of winding in case of separated flux paths.

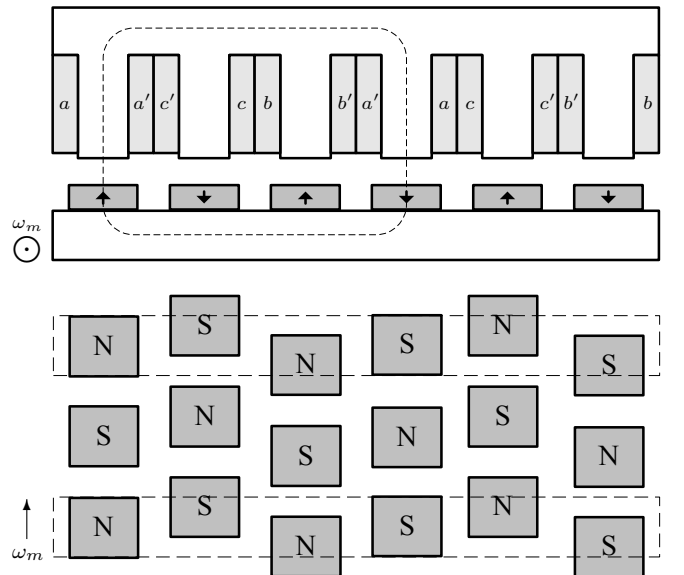


Fig. 5. Arrangement of windings in case of mixed flux paths.

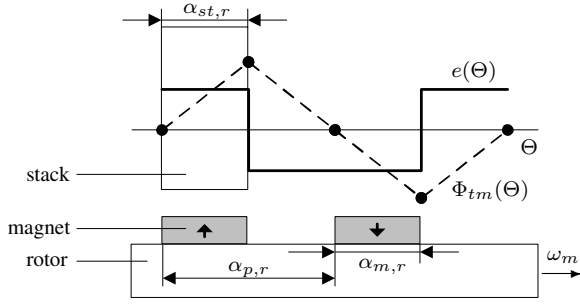


Fig. 6. Distribution of the flux in the teeth Φ_{tm} (dashed line) and induced emf e (solid line) with respect to the angular displacement Θ .

In the case of the separated flux paths (see Fig. 4), the winding has a three-time single phase structure, whereas in the case when the flux paths are mixed (see Fig. 5), the three phase winding distribution is obtained naturally. The windings will be refer to as separated and mixed windings, respectively. The separated windings have shorter end-windings in comparison to the mixed. This offers a possibility of a more compact generator design. The separated winding structure is also easier to analyze. Therefore, the generator with separated winding is analyzed in this paper. The stator slots have a rectangular shape, as well as the conductors in the windings.

C. Induced Emf

The instantaneous value of the induced emf per coil per stator stack is given by

$$e = n_s \frac{d\Phi_{tm}}{dt} = n_s \frac{d\Phi_{tm}}{d\Theta} \frac{d\Theta}{dt} = n_s e(\Theta) \omega_m, \quad (9)$$

where $d\Theta/dt = \omega_m$ is the angular velocity of the rotor, with Θ being the angular displacement, Φ_{tm} is the flux created by the magnets in one tooth, and n_s is the number of conductors in series per winding.

As was mentioned earlier, the dimensions in the rotational plane are subject to changes with respect to the radius R_r , resulting in a variation of the induced emf in different windings. Therefore, the flux variation with the angular displacement should be considered separately for each tooth. The case when $\alpha_{m,r} = \alpha_{st,r}$ and $\alpha_{p,r} = 2\alpha_{m,r}$ is illustrated in Fig. 6 (corresponding to the view depicted in Fig. 3, b). The angular displacement Θ is along the x-axis, Φ_{tm} and e are along the y-axis. The dashed line shows the distribution of $\Phi_{tm}(\Theta)$, whereas the solid line is $e(\Theta)$.

The rms value of the fundamental of the function $e(\Theta)$ is equal to

$$E_{f1} = n_s \omega_m \frac{\alpha_{p,r}}{\sqrt{2}} \int_0^{2\alpha_{p,r}} e(\Theta) \sin\left(\frac{\pi\Theta}{\alpha_{p,r}}\right) d\Theta. \quad (10)$$

Once the type of the winding connection (series, parallel or mixed) is chosen, the phase emf can be calculated.

The output power P_{out} of the generator is given by

$$P_{out} = \eta P_{el} = \eta 3 E_{phase} I_{phase} \cos \phi, \quad (11)$$

where I_{phase} is the phase current, $\cos \phi$ is the power factor, and η is the efficiency of the generator. The three-phase winding is assumed to be a Y-connected.

The total copper losses are defined as

$$P_{cu} = 3 I_{phase}^2 R_{phase}, \quad (12)$$

where R_{phase} is the phase resistance that can be expressed as a function of the winding dimensions as

$$R_{phase} = \rho_{cu} \frac{n_s l_{phase}}{k_{fill} A_{slot}/2} = 2 \rho_{cu} \frac{l_{phase}}{k_{fill} b_{ss} h_{ss}}, \quad (13)$$

where ρ_{cu} is the electric resistivity of copper at winding temperature, $A_{slot} = b_{ss} h_{ss}$ is the slot area, k_{fill} is the slot fill factor, and l_{phase} is the coil length per phase.

The height of the slot can be derived by combining Eqs. 11-13 and setting values for P_{out} , k_{fill} , η , and $\cos \phi$

$$h_{ss} = \frac{2}{3} \frac{\rho_{cu} l_{phase}}{P_{cu} b_{ss} k_{fill}} \left(\frac{P_{out}}{E_{phase} \cos \phi \eta} \right)^2. \quad (14)$$

Once the main dimensions of the machines are determined, the weight of active materials can be calculated.

The total iron losses in the machine can be estimated by the empirical equation provided by [11]

$$P_{fe} = 0.078 W f_e (100 + f_e) B_{ts} G_{fe} \cdot 10^{-3}, \quad (15)$$

where W is the loss factor, $f_e = n_m p / 120$ is the electrical frequency with $n_m = \omega_m 30 / \pi$ the speed of turbine in rpm, and G_{fe} is the weight of laminated iron. The loss factor W is an empirically determined parameter that varies depending on the iron sheet quality, flux density and electrical frequency.

III. PARAMETRIC STUDY

A parametric study was conducted to evaluate the influence of several design parameters on the performances of the generator. The design parameters are presented in Table I. The ratio between induced emf and the active weight G_{total} is an important characteristic that shows how effective the machine active weight is utilized. Besides the total active weight, the weight of the permanent magnets G_{pm} , the most expensive material used in the generator, should be considered separately as it would eventually affect production cost. The predefined parameters for the parametric study are listed in Table II.

TABLE I
DESIGN PARAMETERS

Variable	Value
Main machine radius R_m (m)	1.3
Radii ratio $k_R = R_s / R_m$	0.1
Cut angle ξ (rad)	0.. π
Number of poles p	100..800
Number of teeth per stator stack Q_s	24, 36, 48

TABLE II
PREDEFINED VARIABLES

Property	Value
Output power P_{out} (W)	5 000 000
Power factor $\cos \phi$	0.92
Efficiency η	0.97
Copper losses P_{cu} (W)	$0.02P_{cu}$
Turbine speed n_m (rpm)	13.2
Fill factor k_{fill}	0.55
Number of conductor in series per winding n_s	1
Maximum flux density in the teeth \hat{B}_{ts} (T)	1.4
Airgap flux density B_g (T)	0.9
Magnet remanent flux density $B_{r,pm}$ (T) at 100 °C	1.1
Magnet relative permeability μ_{pm}	1.05

A. Stack and Magnet Dimensions in Rotational Plane

This study was performed in order to investigate how the variation of the dimensions in the rotational plane $l_{st,r}$ and $l_{m,r}$ (or in angular representation $\alpha_{st,r}$ and $\alpha_{m,r}$) affects the analyzed characteristics. The coefficients $k_{mp,r}$ and $k_{stp,r}$ defined in Eqs. 16, 17 are assumed to be varying in the range of 0..1.

$$k_{mp,r} = \frac{\alpha_{m,r}}{\alpha_{p,r}}, \quad (16)$$

$$k_{stp,r} = \frac{\alpha_{st,r}}{\alpha_{p,r}}. \quad (17)$$

Fig. 7, *a* shows the distribution of E_{phase}/G_{pm} and Fig. 7, *b* E_{phase}/G_{total} with respect to $k_{mp,r}$ and $k_{stp,r}$ for the machine with $R_m = 1.65$ m, $R_s = 0.85$ m, $\xi = \pi/3$ rad, $p = 660$, and $Q_s = 36$. The highest values that the examined characteristics can attain when one of the coefficients is fixed and other one is changing are shown in figures with circles. As it can be observed, both ratios have the highest values at $k_{mp,r} = k_{stp,r}$, i.e. when a stack is as thick as a magnet. This observation was supported by the studies that were conducted for different design parameters. Therefore, it was decided to keep these two dimensions equal within the stack sector.

Furthermore, the magnet length in the rotational plane $l_{m,r}$ and the stack plane $l_{m,s}$ were assumed to be approximately 2/3 of the pole pitch $\tau_{p,r}$ and $\tau_{p,s}$, respectively. This would ensure lower leakage between magnets and between stacks in comparison to a full magnet coverage (though no leakage was considered in the model). However, this value of 2/3 should be studied more thoroughly with use of three-dimensional finite element method (FEM) analysis.

B. Number of Poles p

Fig. 8 shows an example of machine with $R_m = 1.65$ m, $Q_s = 36$, $\xi = 1.1574$ rad (66°). In this figure, the machines that had too high iron losses (more than 3% of the output power) were deliberately excluded.

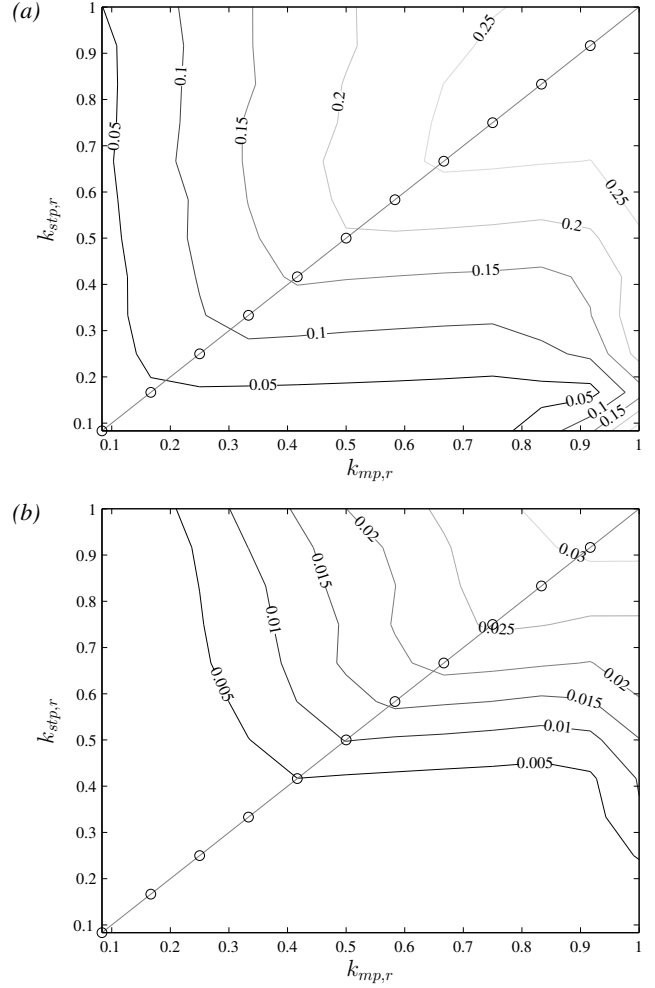


Fig. 7. Distributions of the ratios E_{phase}/G_{pm} (a) and E_{phase}/G_{total} (b) with respect to the coefficients $k_{mp,r}$ and $k_{stp,r}$. Assumed design parameters for the plot are $R_m = 1.65$ m, $R_s = 0.85$ m, $\xi = \pi/3$ rad, $p = 660$.

As anticipated, the TFPM machine characteristics were improving with the increasing number of poles. This is due to the fact that the rate of change of flux is increasing with larger number of poles, while the amount of linking flux is kept unchanged. Therefore, a higher induced emf can be expected for the same mechanical speed. On the other hand, the large number of poles increases the flux leakage, which leads to a poor power factor. This effect is not yet seen here as no leakage was included in the model. Moreover, there are certain mechanical constraints that would limit the maximum allowed stack and magnet thicknesses. By examining different machine geometries, it was found that depending on the main machine radius R_m , the number of poles should be selected in the range of 400..700. However, to find a more appropriate number of poles, three-dimensional FEM analysis is required.

C. Number of Teeth per Stator Stack Q_s

The variation of Q_s in the selected range has shown no considerable impact on the characteristics of the generator. As the cooling is more efficient with smaller slot areas, the

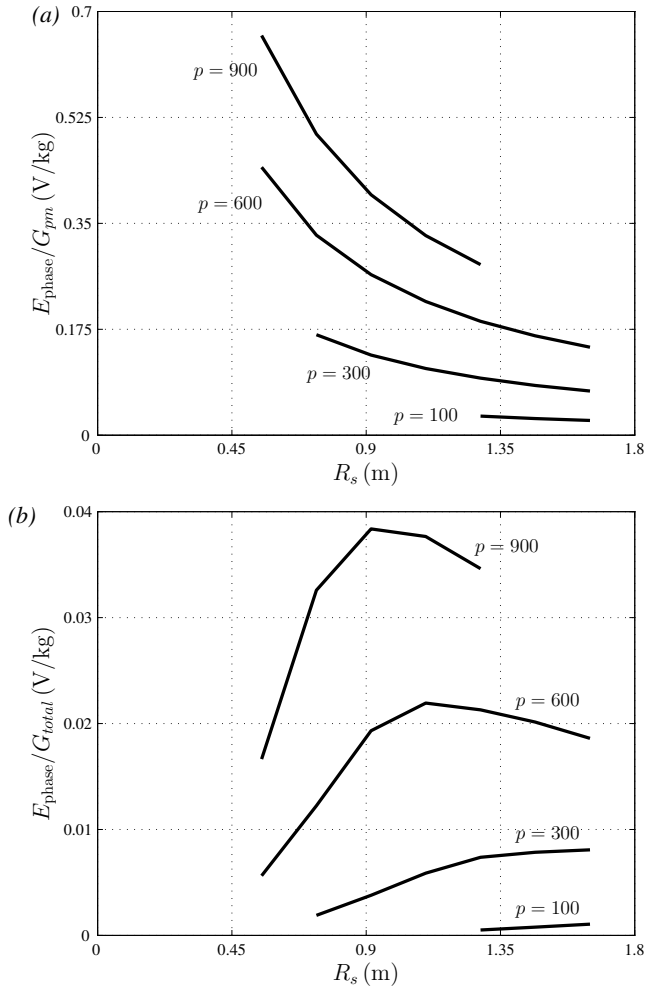


Fig. 8. The number of poles influence on the distributions of E_{phase}/G_{pm} (a) and $E_{\text{phase}}/G_{\text{total}}$ (b) with respect to the tube radius R_s . Assumed design parameters for the plot are $R_m = 1.65$ m, $Q_s = 36$, $\xi = 1.1574$ rad (66°).

number of teeth per stator stack Q_s was chosen equal to 36 in the continuing study.

D. Main Machine Radius R_m , Cut angle ξ , and Radii Ratio k_R

The parametric studies showed that the main machine radius R_m , the tube radius R_s , and the cut angle ξ are interrelated parameters and therefore should be analyzed together.

As it was observed, the low value of R_m would lead to a rather weak generator construction, as the magnets and stacks become relatively thin in the rotational plane, because of the high number of poles. The machine would probably also suffer from the increased leakage, as the distance between the adjoining stacks/magnets would decrease if the number of poles is unchanged. On the other hand, when R_m becomes too large, the machine would considerably increase the nacelle diameter, resulting in a less efficient utilization of the space available in the nacelle. Larger machine diameter would probably also increase the inactive weight of turbine.

For the further analysis, the value of R_m could reasonably

be chosen in the range of 1.5..2 (m). The cut angle ξ and R_s should be selected such as to allow the mechanical coupling of the rotor to the shaft of turbine. These parameters would be selected more properly when the number of poles p and the main machine radius R_m are decided.

IV. CONCLUSIONS

A novel transverse flux permanent magnet generator for the gearless wind turbines has been presented in this paper. The construction features have been described and the analytical design procedure has been presented. The generator seems to have an improved utilization of the materials with the increased number of poles, yet this would lead to lower values of power factor: this tendency is counteracted by increased leakage not yet included in the model. For more proper evaluation of machine performances, the calculation of the leakage flux should be added into the model.

Furthermore, the calculation of inactive weight should be included as well, in order to select the tube radius R_s and the cut angle ξ that give a lower weight of the supporting constructions.

The thermal analysis should also be considered as it allows evaluation of the acceptable level of copper losses. The future work should be concentrated on optimization of the examined generator. Moreover, the analysis for various output power should be performed, as it is believed that the inactive proportion of the nacelle weight of the generator will decrease with the larger output power.

REFERENCES

- [1] *Wind power in power systems*, edited by T. Ackermann, John Wiley & Sons, 2005.
- [2] B.J. Chalmers, W. Wu, and E. Spooner, "An axial-flux permanent-magnet generator for a gearless wind energy system", *IEEE Trans. Energy Conversion*, Vol. 14, No. 2, June, 1999, pp. 251-267.
- [3] H. Polinder, F.F.A. van der Pijl, G.J. de Vilder, and P. Tavner, "Comparison of direct-drive and geared generator concepts for wind turbines", in *Proc IEEE Int. Conf. Electric Machines and Drives*, San Antonio, USA, 2005, pp. 543-550.
- [4] A. Grauers, "Design of direct-driven permanent-magnet generators for wind turbines", PhD thesis, Chalmers University of Technology, Sweden, 1996.
- [5] M.R. Dubois, "Optimized permanent magnet generator topologies for direct-drive wind turbines", PhD thesis, Delft University of Technology, the Netherlands, 2004.
- [6] H. Weh, H. Hoffmann, J. Landrath, "New permanent magnet excited synchronous machine with high efficiency at low speeds", in *Proc. Int. Conf. Electrical Machines*, Vol. 3, Pisa, Italy, 1990, pp. 35-40.
- [7] G. Henneberger and M. Bork, "Development of a new transverse flux motor", *IEE Colloquium on New Topologies for Permanent Magnet Machines*, Digest No. 1997/090, 1997, pp. 1/1-1/6.
- [8] P. Anpalahan, J. Soulard and H.-P. Nee, "Design steps towards a high power factor transverse flux machine", in *Proc. European Conf. on Power Electronics and Applications*, Graz, Austria, 2001.
- [9] H. Weh, H. May, "Achievable force densities for permanent magnet excited machines in new configurations", in *Proc. Int. Conf. Electrical Machines*, Munich, Germany, 1986, pp. 1107-1111.
- [10] H. Polinder, S.W.H. de Haan, M.R. Dubois, and J.G. Slootweg, "Basic operation principles and electrical conversion systems of wind turbines", in *Proc. Nordic Workshop on Power and Industrial Electronics*, Trondheim, Norway, 2004.
- [11] R. Richter, *Elektrische Maschinen*, Bd. IV Basel, Stuttgart: Birkhuser, 1954.